J. Fluid Mech. (1979), *vol.* 95, *part* 4, *pp.* 743–760
Printed in Great Britain

Flow of elastic compressible spheres in tubes

By HÜSNÜ TÖZEREN AND RICHARD SKALAK

Department of Civil Engineering and Engineering Mechanics,
Columbia University, New York, N.Y. 10027

(Received 20 March 1979)

The flow of closely fitting neutrally buoyant elastic spheres through a circular cylindrical tube is considered under the assumptions that the Reynolds' equation is valid in the fluid and equations of linear elasticity hold in the solid. Computations are carried out for several values of Poisson's ratio. The results are compared with the results of previous models on elastic compressible particles.

1. Introduction

The literature on flow of closely fitting particles in tubes has developed largely as models of blood flow in capillaries. The initial studies in this field assumed rigid particles as models of blood cells and axisymmetric Stokes flow [see Goldsmith & Skalak (1975) for references]. These studies showed the geometry of the particle in the vicinity of the tube wall was most important in determining the pressure drop whereas the shape of the rest of the particle and particle spacing had minor influence.

The studies on flow of deformable particles in tubes were initiated by Lighthill (1968) and Fitz-Gerald (1969). They applied lubrication theory to analyse the axisymmetric flow of neutrally buoyant compressible particles in fluid-filled tubes. These compressible particles are assumed to undergo radial deflexions proportional to the local pressure. This model was originally suggested as a model of flow of red cells in narrow capillaries. Tözeren & Skalak (1978) investigated the steady motion of elastic incompressible spheres through cylindrical tubes. Their study was motivated by an interest in the flow of white blood cells in narrow capillary blood vessels.

The present paper is an extension of the previous study under more general assumptions regarding the elastic properties of the particles. Solutions are obtained for several different values of Poisson's ratio and for the range of diameter ratios (particle to tube diameter) between 0·9 and 1·05. The elastic deformations are then of the order of 5 % so the linear theory of elasticity is a reasonable approximation.

The suspending fluid is assumed to be incompressible and Newtonian. Inertial effects are neglected and only neutrally buoyant particles are considered. The fluid layer between the particle and the tube is assumed to be sufficiently small so that Stokes equation can be reduced to the Reynolds equation. The lubrication theory is known to give accurate results for closely fitting rigid particles (Skalak *et al.* 1972).

In § 2 the Reynolds equation is formulated and a series solution for displacements of elastic spheres is developed. In § 3, the numerical results are discussed and compared with the model due to Lighthill (1968) and Fitz-Gerald (1969).

0022-1120/79/4349-7930 $02.00

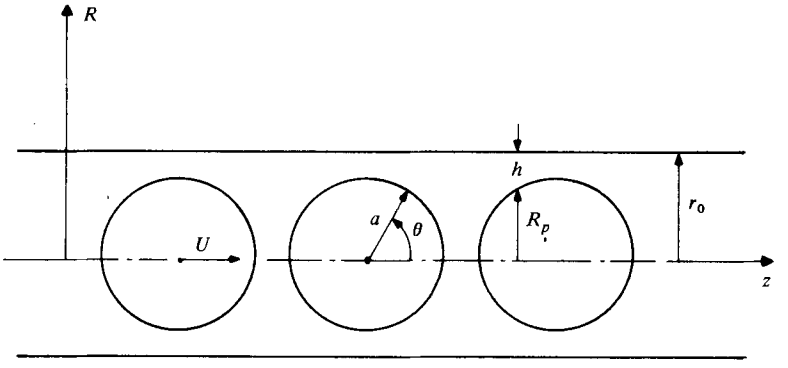

FIGURE 1. Elastic particles having a spherical shape in the unstressed state translate concentrically through a circular cylinder.

2. Formulation

Consider a line of spherical particles of radius a when unstressed, located axisymmetrically in a tube of radius r_0 (figure 1). In a previous paper (Tözeren & Skalak 1978) it was shown that a unique solution can be found for incompressible particles for given initial diameter ratio a/r_0, shear modulus G, fluid viscosity μ, and pressure drop across the particle Δp. The solutions apply for any case of a given Δp, even though the mean pressure varies, say by raising both upstream and downstream pressure equally.

The case of compressible particles to be treated here differs from the incompressible case in that a change of the mean pressure level changes the volume and radius of the particles. A uniform pressure p' produces a radial displacement $-(p'/3\kappa)a'$ of the surface of an elastic sphere, where a' denotes the initial radius of the sphere and κ is its bulk modulus. Now consider such a sphere in a tube and suppose that for some specified values of a/r_0, μ, G, κ and Δp it happens that mean pressure on the sphere vanishes so $p_m = 0$. This solution may also be used to solve certain cases with $p_m \neq 0$. Suppose there is a sphere of radius a' (when unstressed) related to the solution above by

$$a' = a(1+p_m/3\kappa), \tag{2.1}$$

where p_m is a mean pressure different from zero. The solution for the same G, κ, μ and Δp as before will be U, V and

$$\mathbf{u}' = \mathbf{u} - (p_m/3\kappa)\, a\mathbf{e}_r, \tag{2.2}$$

where U, V and $\mathbf{u}$ are the solutions with $p_m = 0$ mentioned above. This use of the solutions with $p_m = 0$ is permissible because the displacements are superposable under the assumptions of theory of linear elasticity. This point will be further considered in § 3. The formulation below is given under the assumption that $p_m = 0$. A family of such solutions is sufficient to evaluate all cases with $p_m \neq 0$ also.

The Reynolds number in microcirculation is typically of the order of 10^{-3} and hence the fluid inertial terms are negligible. The motion of suspending fluid is considered to be a steady Stokes flow relative to the particle. The fluid film thickness between the particle and the tube is assumed to be small compared to tube radius. Under this

assumption the Stokes equations and the equations of continuity can be reduced to the Reynolds equation (Fitz-Gerald 1969). When referred to the cylindrical co-ordinate system (R, ϕ, z) fixed relative to the particle the Reynolds equation is (Tözeren & Skalak 1978)

$$\frac{dp}{dz} = \left[r_0 Q - U\left(\tfrac{1}{2}r_0^2 + \frac{2r_0h - h^2}{4\ln(1-h/r_0)}\right)\right]\left[\frac{2r_0h-h^2}{16\mu}\right]^{-1} \times \left[2r_0^2 - 2r_0h + h^2 + \frac{2r_0h-h^2}{\ln(1-h/r_0)}\right]^{-1}, \quad (2.3)$$

where r_0 is the tube radius, h is the thickness of the lubrication layer, U is the particle velocity and

$$Q = \tfrac{1}{2}r_0(U - V) \quad (2.4)$$

is the leakback.

It is assumed that the resultant force on the particle due to pressures and viscous stresses exerted by the fluid is equal to zero. This condition of zero drag on the neutrally buoyant particle is formulated by considering the equilibrium of a control volume bounded by the tube wall, particle surface and two planes tangential to the particle at the downstream and upstream ends (Tözeren & Skalak 1978):

$$\pi r_0^2[p(-a) - p(a)] = 2\pi \int_{-a}^{a} r_0[\tau_{Rz}]_{R=r_0}\, dz. \quad (2.5)$$

The solutions of equations of equilibrium of an elastic sphere in terms of series of spherical harmonics were considered by Love (1944). The series expansion for displacement $\mathbf{u}$ of an elastic sphere subject to purely radial surface tractions are given in §§ 172 and 173 (ii) of Love (1944). The problem of an elastic sphere subject to purely tangential surface tractions can be treated similarly. The relationship between the solid spherical harmonics ω_n and ϕ_n which are used to express $\mathbf{u}$ (equations (172.5) and (172.8) of Love (1944)] and the stress vector $\mathbf{P}_r$ acting across a spherical surface with radius a can be found by solving the equation

$$\mathbf{P}_r \cdot \mathbf{e}_r = 0 \quad \text{on} \quad r = a, \quad (2.6)$$

where $\mathbf{e}_r$ is the unit radial vector. Substitutions of Love's equations (172.12) and (172.13) which express $\mathbf{P}_r$ in terms of ω_n and ϕ_n in (2.6) yields the relationship between ω_n and ϕ_n in this case as

$$\phi_n = D(n)\, a^2 \omega_n,$$

where

$$D(n) = -\frac{n(2n+\alpha_n) + 2n((\lambda/G)+1) + \alpha_n\{(n+3)(\lambda/G) + (n+2)\}}{2n(n-1)}; \quad (2.7)$$

α_n is defined by (172.7) of Love (1944), λ is the first Lamé constant and G is the shear modulus of the elastic particle.

In the case of axisymmetric deformations, the harmonic functions ω_n and ϕ_n can be written as

$$\omega_n = \gamma_n (r/a)^n P_n(\cos\theta), \quad (2.8)$$

$$\phi_n = \beta_n (r/a)^n P_n(\cos\theta), \quad (2.9)$$

in spherical co-ordinates (r, θ, ϕ), where $P_n(\cos\theta)$ is the Legendre function of order n.

When the tangential surface tractions $P_{r\theta}$ are specified, the coefficients of the series expansion of $P_{r\theta}$ in terms of derivatives of Legendre functions can be used to determine γ_n and β_n. Let

$$P_{r\theta}\operatorname{cosec}\theta = G\sum_{n=1}^{\infty} A_n \frac{\Gamma(n+1)}{\Gamma(n+3)} P'_{n+1}(\cos\theta), \tag{2.10}$$

where

$$A_n = \frac{2n+3}{2}\int_0^{\pi} P_{r\theta}\sin\theta P'_{n+1}(\cos\theta)\,d(\cos\theta), \tag{2.11}$$

and Γ is the gamma function. Then using equations (172.12) and (172.13) of Love (1944),

$$\gamma_n = -\frac{A_{n-1}}{(n+1)E(n)}, \tag{2.12}$$

where $E(n)$ is given by

$$E(n) = 2n(\lambda/G+1)+\alpha_n\{(n+3)\lambda/G+(n+2)\}, \tag{2.13}$$

and the displacement $\mathbf{u}$ at $r = a$ can be found as

$$\mathbf{u} = a\sum_{n=2}^{\infty}\{(1+D(n))\gamma_n\{(P'_n\mathbf{e}_z - P'_{n-1}\mathbf{e}_r\}+\alpha_n\gamma_n P_n\mathbf{e}_r\} \tag{2.14}$$

at $r = a$ by substituting (2.7)–(2.9) and (2.12) into (172.5) and (172.8) of Love (1944).

The solution for an elastic sphere with purely radial surface tractions is given in § 173 (ii) of Love (1944) as

$$GE(n)\,\omega_n = B_n\left(\frac{r}{a}\right)^n P_n, \quad \phi_n = -\frac{2n+\alpha_n}{2(n-1)}a^2\omega_n \tag{2.15}$$

for $n \neq 1$, where B_n is the coefficient of $P_n(\cos\theta)$ in the Legendre series expansion for radial surface tractions.

The terms of first degree are not included in (2.10) and (2.15). These are the only components in the series expansions which would have non-zero resultant on the particle. The resultants of normal and tangential tractions are equal and opposite if the condition of zero drag on the particle is satisfied. The solutions for this case can be obtained from the equations given in § 173 (i) of Love (1944) by setting $n = 1$:

$$\mathbf{u} = \alpha_n a\omega_n\mathbf{e}_r \quad \text{at} \quad r = a, \tag{2.16}$$

$$\mathbf{P}_r = G(2+\alpha_n)a\nabla\omega_n + GE(n)(\mathbf{r}/a)\omega_n \quad \text{at} \quad r = a, \tag{2.17}$$

where $E(n)$ is defined by (2.13).

The preceding equations are non-dimensionalized by using the following dimensionless variables:

$\tilde{\mathbf{r}} = \mathbf{r}/a$ = dimensionless position vector,

$\tilde{h} = h/r_0$ = dimensionless clearance,

$\tilde{p} = p/G$ = dimensionless fluid pressure,

$\tilde{\sigma}_{ij} = \sigma_{ij}/G$ = dimensionless stress tensor,

and the dimensionless parameters

$A = \mu Ua/Gr_0^2$ = velocity parameter,

$\lambda_i = a/r_0$ = initial diameter ratio,

$C = 2Q/Ur_0$ = leakback parameter.

The Reynolds equation and condition of zero drag in dimensionless form are

$$\frac{d\tilde{p}}{d\tilde{z}} = 8A\left(C-\left(1+\frac{(2-\tilde{h})\tilde{h}}{2\ln(1-\tilde{h})}\right)\right)\left(2-2\tilde{h}+\tilde{h}^2+\frac{\tilde{h}(2-\tilde{h})}{\ln(1-\tilde{h})}\right)^{-1}(\tilde{h}(2-\tilde{h}))^{-1}, \tag{2.18}$$

$$\Delta\tilde{p} = \int_{-1}^{1}\left\{\frac{1}{2}\frac{d\tilde{p}}{d\tilde{z}}\left(2+\frac{\tilde{h}(2-\tilde{h})}{\ln(1-\tilde{h})}\right)+\frac{2A}{\ln(1-\tilde{h})}\right\}d\tilde{z}. \tag{2.19}$$

Equations (2.10)–(2.19) are coupled by the requirements that:

(i) along the particle surface the stress vector is continuous

$$\mathbf{n}.\boldsymbol{\sigma}_s = \mathbf{n}.\boldsymbol{\sigma}_f, \tag{2.20}$$

where $\mathbf{n}$ is the unit normal vector on the surface and s and f indicate solid and fluid regions;

(ii) the gap thickness h is dependent on the surface displacements

$$h = r_0 - R_p - u_R, \tag{2.21}$$

where R_p is the radial co-ordinate of the undeformed particle surface and u_R is the displacement in R direction along $R = R_p$ surface. In (2.21) the axial deflexion is neglected on grounds that the slopes involved are small.

The system of equations (2.10)–(2.19) may be solved by a procedure of successive approximations for the unknowns: the displacement vector $\tilde{\mathbf{u}}$, dimensionless pressure $\tilde{p}$ and A or C whichever is not specified.

In order to start the numerical iteration procedure, suppose that the steady-state surface shape of the particle is estimated. Then, the Reynolds equation (2.18), the condition of zero drag (2.19) can be solved under the condition that the mean pressure is equal to zero to yield the pressures and viscous stresses in the fluid. These stresses are then applied to the particle and the displacements are re-computed. The particle thus may attain a different surface shape than the previous approximation. A combination of previous and current surface shapes which facilitates numerical stability is then adopted for the determination of pressures at the next step of successive approximations. The computational cycle is repeated until the changes in displacements become sufficiently small compared to the magnitude of the current approximation to the displacements.

3. Numerical results

The numerical procedure formulated in § 2 is used to study the motion of elastic spheres for the particular cases of Poisson's ratio $\sigma = 0$ and $\sigma = \frac{1}{4}$. The incompressible elastic particle case ($\sigma = \frac{1}{2}$) was treated previously by Tözeren & Skalak (1978). The initial diameter ratio λ_i and the velocity parameter A are specified and the deformations of the elastic particle, the leakback parameter C and the dimensionless pressure drop $\Delta\tilde{p}$ are computed. The computations are carried out under the condition $p_m = 0$ as mentioned in § 2. However, the superposition principle of linear elasticity makes it possible to use the numerical results for this case in solving cases which involve non-zero mean pressure. This will be illustrated below.

In addition to the dimensionless parameters defined earlier, the relative apparent viscosity defined by

$$\eta = \Delta p/(16\mu Va/r_0^2) \tag{3.1}$$

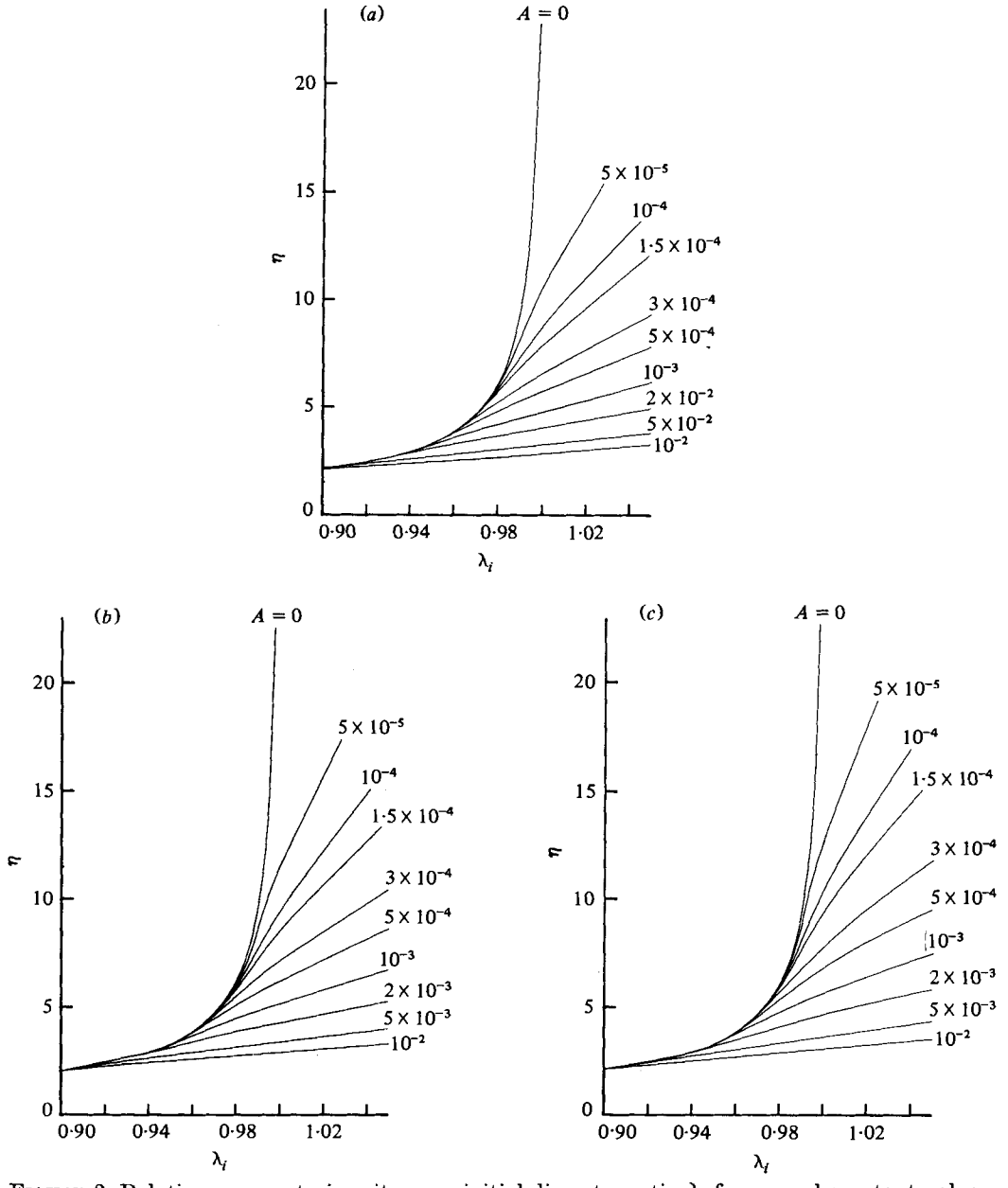

FIGURE 2. Relative apparent viscosity η *vs.* initial diameter ratio λ_i for several constant values of A. The spacing between the particles is one particle diameter $d = 2a$ and the mean pressure on the particle is equal to zero $p_m = 0$. (*a*) $\sigma = 0$; (*b*) $\sigma = \frac{1}{4}$; (*c*) $\sigma = \frac{1}{2}$ (incompressible particles).

is used in presentation of the numerical results. As defined by (3.1), η applies to a line of spheres in contact with each other. The η for arbitrary particle spacings can be approximated by averaging the results given here for a line of spheres that are just touching each other with $\eta = 1$ for the spaces between the particles.

Figure 2 shows η as a function of A and λ_i for $\sigma = 0$, $\frac{1}{4}$ and $\frac{1}{2}$ respectively. A numerical error in computer programs used by Tözeren & Skalak (1978) is corrected so figure 4

of that paper differs slightly from figure 1 (*c*). The curve $A = 0$ gives the solutions for a rigid sphere. The differences between A = constant curves increase for higher values of λ_i for all σ. This is due to the elastic deformations of the particle, which are much larger than the thickness of the fluid film for greater values of λ_i. For fixed A and λ_i, the values of η decrease as σ decreases from $\frac{1}{2}$ to 0. For example, for $\lambda_i = 1{\cdot}04$ and $A = 10^{-4}$, the η values are approximately 17, 15 and 13 for $\sigma = \frac{1}{2}, \frac{1}{4}$ and 0 respectively. The differences between these curves would have decreased if Young's modulus E rather than shear modulus G were used in non-dimensionalization as the first parameter involving elasticity. The value of E ($E = 2(1+\sigma)G$) increases by a factor of $\frac{3}{2}$ as σ varies between 0 and $\frac{1}{2}$ for a fixed value of G. For example, for the fixed value of $(\mu Ua/Er_0^2) = 0{\cdot}5 \times 10^{-4}$ ($A = (\mu Ua/Gr_0^2) = 10^{-4}$ for $\sigma = 0$) and $\lambda_i = 1{\cdot}04$, η is equal to 14·5, 14 and 13 for $\sigma = \frac{1}{2}, \frac{1}{4}$ and 0. So, it appears that the behaviour of the curves is strongly dependent on E but not on σ. This behaviour is similar to the case of contact between elastic bodies in which the deformation is dependent on the elastic properties through a factor $(1-\sigma^2)/E$ [see equation (138.57), Love (1944)]. This factor varies only 25 % for E fixed and $0 < \sigma < \frac{1}{2}$. In the present case, the results are not exactly proportional to $(1-\sigma^2)/E$; but we certainly expect this to be a reasonable approximation when (i) A is very small ($G \to \infty$), (ii) a is slightly greater than r_0 so the dimensions of the contact (compressed) area are very small and (iii) the gap thickness is much smaller than the displacements of the particle in contact area. Under these conditions, there have been successful applications of contact theory of elasticity to lubrication problems (Cameron 1966).

The curves of C *versus* λ_i for constant values of A are shown in figure 3 for $\sigma = 0, \frac{1}{4}$ and $\frac{1}{2}$. The average velocity V is equal to $U(1-C)$ so when U is given these curves can be used to determine V. For smaller values of λ_i the elastic deformations are much less compared to the thickness of the fluid film. Hence, all C *versus* λ_i curves approach the curve for rigid spheres ($A = 0$) which may be approximated by using the asymptotic relation between C and $\tilde{h} = 1-\lambda_i$ derived by Bungay & Brenner (1973) for rigid spheres:

$$C = \tfrac{4}{3}\tilde{h} - \tfrac{46}{15}\tilde{h}^2 + O(\tilde{h}^3) \quad \text{as} \quad \tilde{h} \to 0. \tag{3.2}$$

Some information about particle deformations and fluid film thicknesses is given in figure 4. The variable λ_f is the maximum radius of the particle after deformations non-dimensionalized by r_0. The $A = 0$ curves corresponding to rigid spheres are 45° straight lines (no deformation). The difference between this line and A = constant curves gives the elastic displacement approximately at the location where fluid film thickness is minimum. This minimum film thickness is given by the difference between $\lambda_f = 1$ line and A = constant curves. For a constant A, the value of λ_f decreases as σ decreases from $\frac{1}{2}$ to 0. The difference between these curves would be reduced if E rather than G were used in definition of A according to the discussion given above. As λ_i decreases, all A = constant curves approach the $A = 0$ line. For higher values of λ_i the elastic deformations become greater and $(\lambda_i - \lambda_f)$ increase. The successive approximation procedure described in § 2 is not convergent when $\tilde{h}$ is less than 0·005 (or $\lambda_f > 0{\cdot}995$). It is therefore not possible to make a definitive statement whether or not λ_f ever becomes equal to unity, in which case η would be infinite. It would be more appropriate to use the contact theory of elasticity to investigate this limit. Such an approach would be valid in the vicinity of the corner where the $A = 0$ curves intersect the line $\lambda_f = 1$.

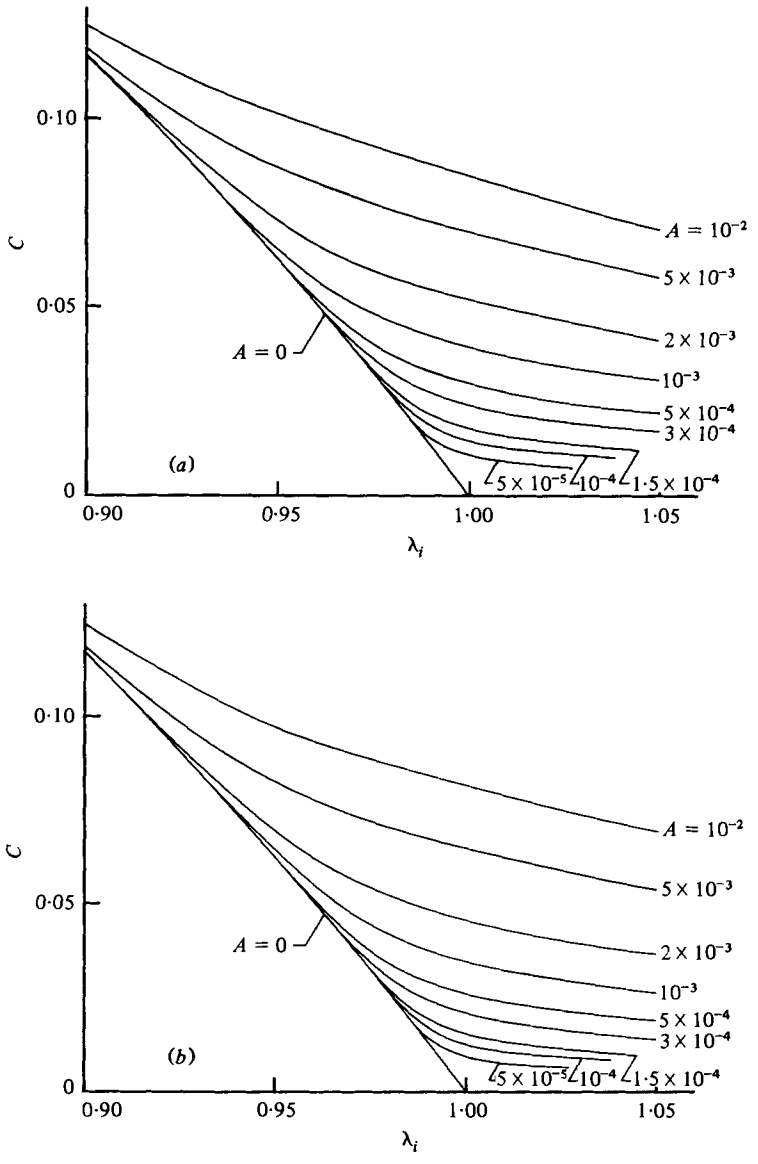

FIGURE 3. For legend see facing page.

The other two sets of curves of interest are η *versus* λ_i and $\tilde{p}(-a)$ *versus* λ_i for for $\Delta\tilde{p}$ = constant curves shown in figures 5 and 6. These curves are convenient to solve certain physical problems. Before giving specific examples, these curves will be discussed briefly.

The η *versus* λ_i for $\Delta\tilde{p}$ = constant curves are similar to curves given in figure 2. For fixed λ_i and $\Delta\tilde{p}$, the drag on the elastic particle is greater for higher values of σ. These curves show that for a fixed $\Delta\tilde{p}$ both η and the derivative of η with respect to λ_i increase as λ_i increases; so there may be a limiting λ_i^* for a fixed $\Delta\tilde{p}$ that η may tend to infinity while $\Delta\tilde{p}$ = constant. The curve would have a vertical asymptote $\lambda_i = \lambda_i^*$ for which λ_f would asymptotically tend to 1.

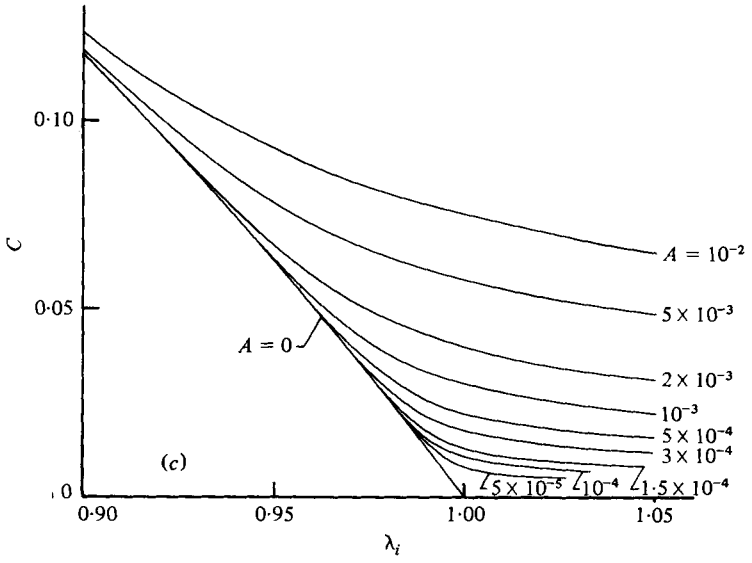

FIGURE 3. The leakback parameter $C = 2Q/Ur$ *vs.* initial diameter ratio λ_i for constant values of A. The mean pressure on the sphere is equal to zero, $p_m = 0$. (*a*) $\sigma = 0$; (*b*) $\sigma = \frac{1}{4}$; (*c*) $\sigma = \frac{1}{2}$ (incompressible particles).

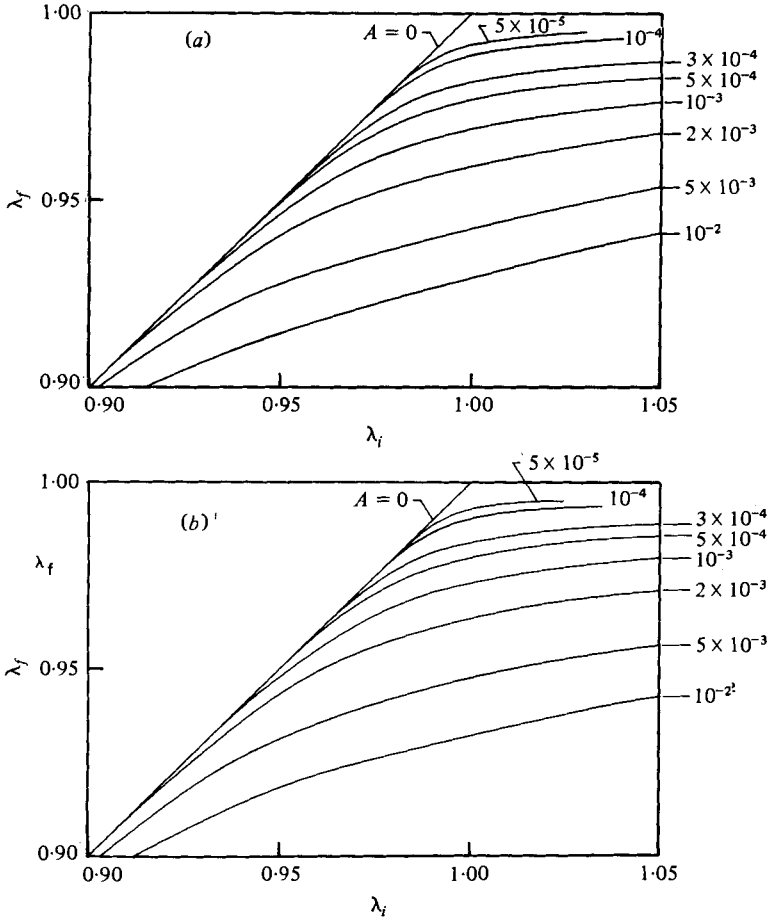

FIGURE 4. For legend see overleaf.

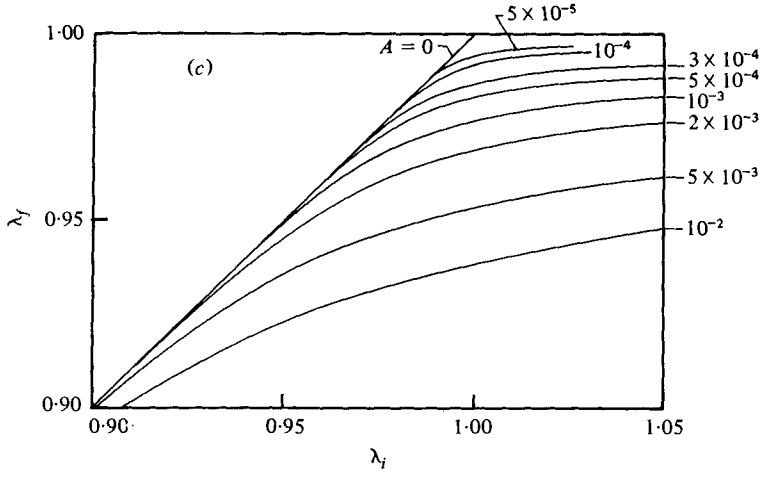

FIGURE 4. The final diameter ratio λ_f *vs.* initial diameter ratio λ_i for several values of A. The curves are obtained under the assumption that $p_m = 0$. (*a*) $\sigma = 0$; (*b*) $\sigma = \frac{1}{4}$; (*c*) $\sigma = \frac{1}{2}$ (incompressible particles).

It was mentioned above that all the curves are obtained for the case $p_m = 0$. In this case the upstream pressure (the initial condition for pressure when integrating the Reynolds equation) may not be specified arbitrarily. The information regarding the upstream pressure $\tilde{p}(-a)$ is given in figure 6(*a*) and (*b*) for $\sigma = 0$ and $\frac{1}{4}$. For a rigid sphere, if $\tilde{p}(-a)$ is chosen as $\frac{1}{2}\Delta\tilde{p}$ the lubrication pressures would be antisymmetric with respect to origin due to the symmetry. Hence $p_m = 0$ for this case. Accordingly, for λ_i small (when elastic deformations are small) all $\tilde{p}(-a)$ *versus* λ_i curves (for fixed $\Delta\tilde{p}$) approach to $\tilde{p}(-a) = \frac{1}{2}\Delta\tilde{p}$. But the pressure curves for greater λ_i values (see figures 2 and 7 of Tözeren & Skalak, 1978) are less symmetric than those of rigid spheres. In these cases there is a pressure buildup especially in a region where particle radius is greater than tube radius to produce the required deformations of the particle. Hence, in order to satisfy the condition $p_m = 0$, the integration of Reynold's equation must be started with negative values for upstream pressure ($\tilde{p}(-a) < 0$). This explains the small negative regions of figures 6(*a*) and (*b*).

A numerical example is solved below to demonstrate how figures 5 and 6 and the superposition principle are used in solving numerical problems.

Let the material constants, initial particle and tube geometry and pressure drop be specified. The particle velocity, average velocity and minimum gap thickness are to be determined. The material constants are:

$$G = 10^5 \text{ dyne/cm}^2, \quad \mu = 1{\cdot}2 \times 10^{-2} \text{ poise},$$
$$\sigma = \tfrac{1}{4},$$
$$\Delta p = 5 \times 10^3 \text{ dyne/cm}^2 \approx 5 \text{ cmH}_2\text{O},$$
$$p_u = \text{upstream pressure} = 1{\cdot}25 \times 10^4 \text{ dyne/cm}^2,$$
$$a' = \text{particle radius} = 4{\cdot}2\,\mu\text{m} = 4{\cdot}2 \times 10^{-4} \text{ cm},$$
$$r_0 = \text{tube radius} = 4 \times 10^{-4} \text{ cm},$$
$$a'/r_0 = 1{\cdot}05.$$

(These values are in the range of a white blood cell in a small capillary blood vessel.)

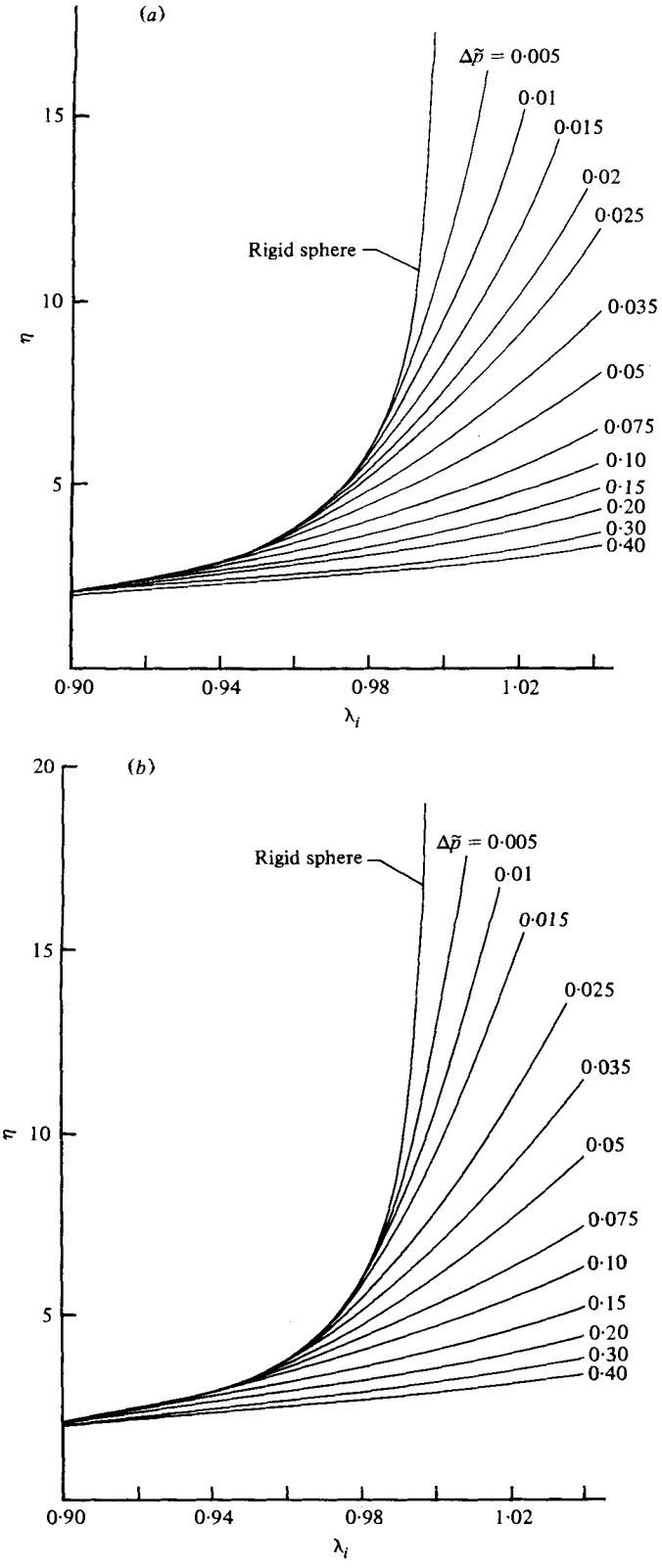

FIGURE 5. For legend see overleaf.

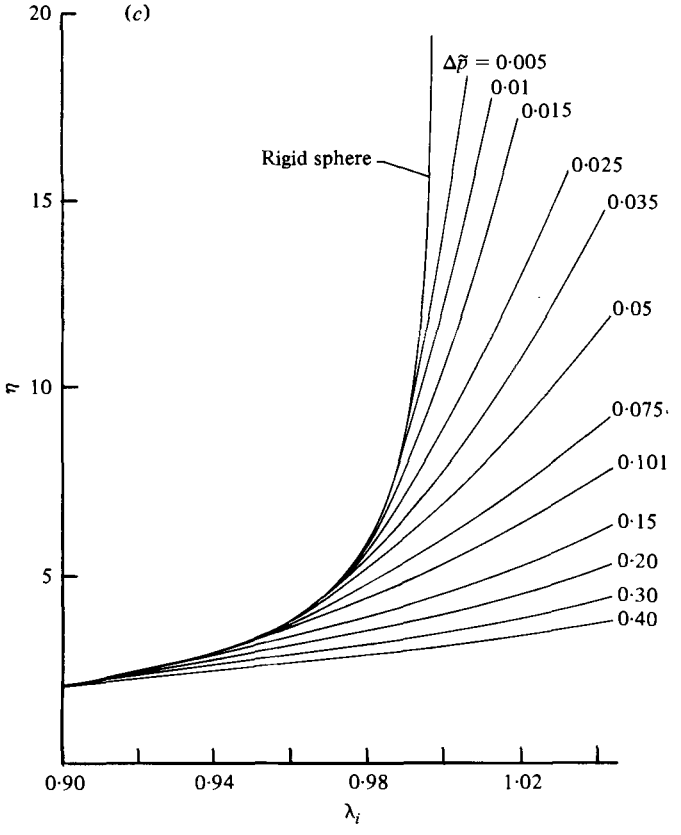

FIGURE 5. The relative apparent viscosity η as a function of initial diameter ratio λ_i and dimensionless pressure drop $\Delta p = \Delta\tilde{p}/G$. The spacing between the particles is one particle diameter $d = 2a$ and the mean pressure on the particle is equal to zero, $p_m = 0$. (*a*) $\sigma = 0$; (*b*) $\sigma = \frac{1}{4}$; (*c*) $\sigma = \frac{1}{2}$ (incompressible particles).

Let p_m be the unknown mean pressure. Under p_m the particle with radius a' will deform and assume a new radius a

$$\frac{a}{r_0} = \frac{a'}{r_0}\left(1 - \frac{p_m}{3\kappa}\right) \tag{3.3}$$

or in this particular case using $3\kappa = \frac{1}{5}G$,

$$\lambda_i = \frac{a'}{r_0}\left(1 - \frac{\tilde{p}_m}{5}\right). \tag{3.4}$$

Consider now the rest of the lubrication pressures (with mean equal to zero) having an upstream value as the unknown $p(-a)$. The addition of $p(-a)$ to p_m must give p_u:

$$p_m = p_u - p(-a). \tag{3.5}$$

Substituting (3.5) into (3.4), one equation in two unknowns λ_i and $\tilde{p}(-a)$ is obtained. The other equation involving λ_i and $\tilde{p}(-a)$ is given by $\Delta\tilde{p} = 0{\cdot}05$ curve of figure 6(*b*). The solution of these two equations by trial and error yield

$$\lambda_i = 1{\cdot}0195, \quad \tilde{p}(-a) = -0{\cdot}0195.$$

Using η *versus* λ_i curve $\Delta\tilde{p} = 0{\cdot}05$ (figure 5*b*) and $\lambda_i = 1{\cdot}0195$, η can be found as 7·5. Then, using the η *versus* λ_i curve for fixed A (figure 2*b*) for $\eta = 7{\cdot}5$ and $\lambda_i = 1{\cdot}0195$ A can be determined:

$$A = 4{\cdot}481 \times 10^{-4}.$$

The use of figure 3(*b*) and figure 4(*b*) for $A = 4{\cdot}481 \times 10^{-4}$ and $\lambda_i = 1{\cdot}0195$ yields

$$C = 0{\cdot}0207 \quad \text{and} \quad \lambda_f = 0{\cdot}9844.$$

Then

$$U = \frac{AGr_0^2}{\mu a} = 1{\cdot}423\ \text{cm/s}^{-1},$$

$$V = U(1-C) = 1{\cdot}394\ \text{cm s}^{-1}$$

and

$$h = (1-\lambda_f)a = 6{\cdot}552 \times 10^{-2}\,\mu\text{m}.$$

These velocities are high for blood flow, but they illustrate the procedure. With most other combinations of initial data, the solutions using the curves will be found to be more direct. It is of interest to compare the results obtained above with the studies of Lighthill (1968) and Fitz-Gerald (1969). An error in their formulation of zero-drag condition was pointed out previously (Tözeren & Skalak 1978). The capillary flow for their model is solved using the correct zero-drag condition and extensive numerical results are obtained below. Some dimensionless variables used in their studies are

$$\left.\begin{aligned} A' &= \mu U\beta/r_0^2(kr_0)^{\frac{1}{2}}, \\ D' &= [p(-g) - p(g)]\,r_0(kr_0)^{\frac{1}{2}}/\mu U, \\ F' &= \frac{\beta}{r_0}\left[\frac{p(g)+p(-g)}{2} - p_0\right] \\ \text{and} \quad P(-G) &= \frac{\beta(p(-g)-p_0)}{2Q/U}, \end{aligned}\right\} \tag{3.6}$$

where β = compliance of the particle, k = the curvature at the point of contact between the tube and the particle, p_0 = the reference pressure, and $-g$ = co-ordinate of upstream end of the particle.

The dimensionless upstream pressure $P(-G)$ *versus* A' curves for constant values of C are given in figure 7. This information about $P(-G)$ is important because when A and C are specified, the lubrication pressures (and shear stresses) obtained by integrating Reynolds' equation using as initial condition the $P(-G)$ obtained from figure 7 satisfy the zero-drag condition.

Figure 8 shows D' *versus* F' curves for constant values of A' and of C. Some of these curves were given by Tözeren & Skalak (1978) in figure 3. Figure 8 gives more extensive data.

To compare the results of corrected Lighthill–Fitz-Gerald theory of figures 7 and 8 to the elastic sphere solutions, it is necessary to recast the latter in similar dimensionless variables. For fixed A and C, it is shown above that the solutions for an elastic sphere under the condition $p_m = 0$ can be generalized to elastic spheres of different sizes if the upstream pressure is adjusted accordingly. The sphere with radius equal to r_0 is included in this group. The uniform pressure required to deform a sphere with radius r_0 into a sphere with radius a is given as [see equation (3.3)]:

$$p'_m = 3\kappa(1-a/r_0). \tag{3.7}$$

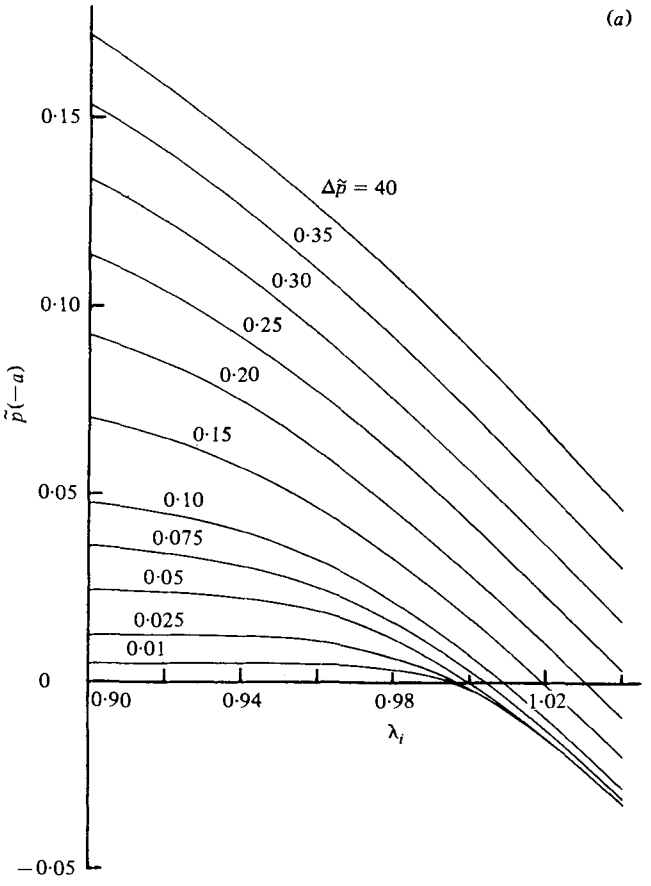

FIGURE 6. For legend see facing page.

Let $p(-a)$ and $p'(-a)$ denote the upstream pressures for (i) the sphere with radius a ($p_m = 0$) and (ii) the sphere with radius r_0 ($p_m = p'_m$). The difference between these pressures must be equal to the mean pressure in the second case:

$$p'(-a) = p'_m + p(-a). \tag{3.8}$$

Using (3.7) and (3.8)

$$p'(-a) - p(-a) = 3\kappa(1-\lambda_i). \tag{3.9}$$

Then, it is possible to calculate the analogue of F' by using (3.9) and figure 6:

$$F = (p'(-a) + p'(a))/2G, \tag{3.10}$$

where $p'(a) = p'(-a) + \Delta p$ and using G in (3.10) in place of β/r_0 in (3.6). The formulation of D in terms of dimensionless parameters used in this study is more straightforward: Define

$$D = \Delta p/(\mu U/r_0) = (\Delta\tilde{p}/A)\lambda_i. \tag{3.11}$$

In (3.11) we need only to identify $k = r_0^{-1}$ for a sphere to correlate with (3.6). Using the definitions (3.10), (3.11), the curves in figure 2 involving parameters λ_i and η can be converted into D *versus* F curves for A = constant. The A, F and D used here are all similar parameters to Lighthill's A', F' and D'; the only difference is here G rather than r_0/β is used in the definition of the dimensionless parameters.

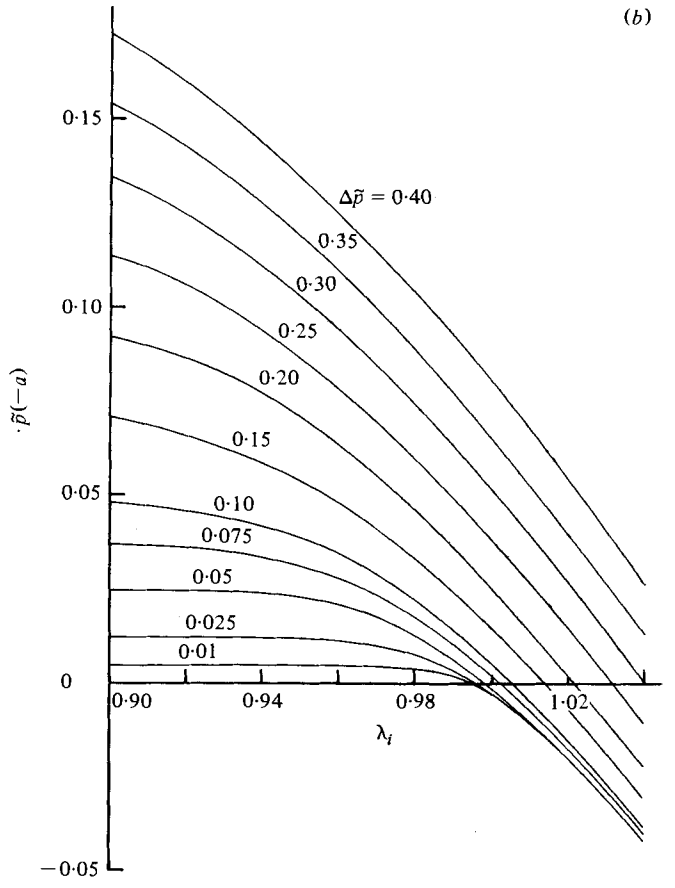

FIGURE 6. The dimensionless upstream pressure $\tilde{p}(-a)$ as a function of initial diameter ratio λ_i and dimensionless pressure drop $\Delta\tilde{p}$. The mean pressure p_m on the particle is equal to zero. (*a*) $\sigma = 0$; (*b*) $\sigma = \frac{1}{4}$.

Figures 9 and 10 show *F versus D* curves for several values of A and for $\sigma = 0$ (figure 9) and $\sigma = \frac{1}{4}$ (figure 10). Although the range of D is the same, the curves for elastic compressible particles (figures 9 and 10) which are concave downwards differ from the corresponding curves for the model of Lighthill (1968) and Fitz-Gerald (1969) which are concave upwards shown in figure 8. The reason is that the linear relationship between the pressures and radial deflexions used in their model is not a good approximation for elastic particles even in the vicinity of the point where the film thickness attains its minimum.

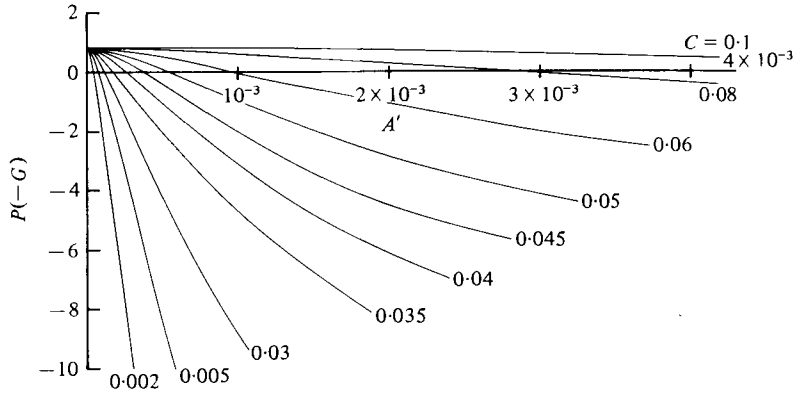

FIGURE 7. The dimensionless upstream pressure $P(-G)$ as a function of A' and C.

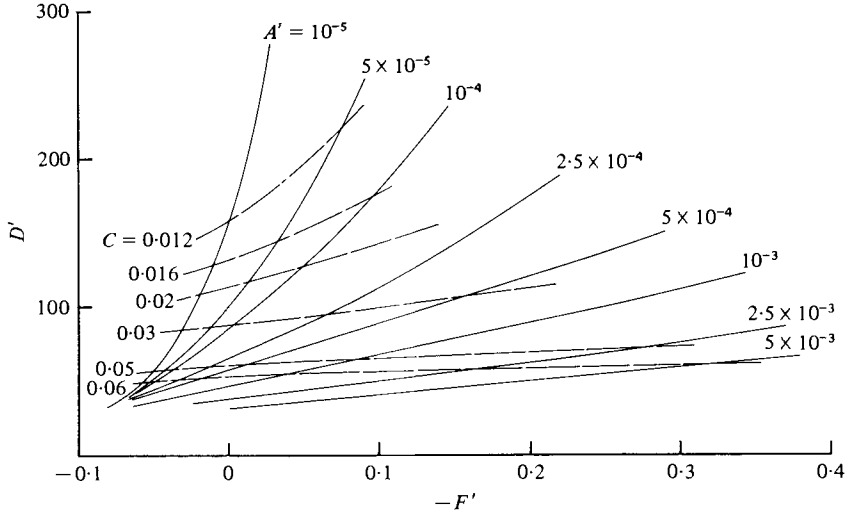

FIGURE 8. The D' *vs.* F' curves for several constant values of A' and C.

The above comparison indicates that the parameter, F, introduced by Lighthill and Fitz-Gerald is analogous to the unstressed diameter ratio, λ_i, used in the present paper. The use of the parameters of Lighthill and Fitz-Gerald or the set used in the present paper is optional in the sense that the general case of any initial size of particle and mean pressure may be treated using the curves for either formulation presented above by the appropriate superpositions of mean pressure.

The results of the corrected Lighthill–Fitz-Gerald theory (figure 8) are of the same order of magnitude as the present results for elastic spheres when similar parameter values are used (figures 9 and 10). However, there is a qualitative difference for particles which are larger than the tube when unstressed ($F < 0$ in figures 8–10) in that the curvature of the curves for A' = constant in figure 8 is of opposite sign to that for A = constant in figures 9 and 10. An exact comparison is not possible because the choice of particle stiffness β (in the Lighthill–Fitz-Gerald theory) which is equivalent

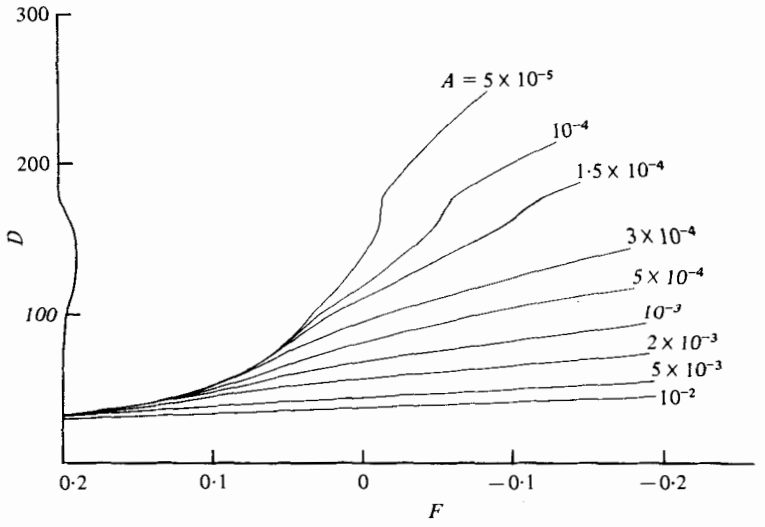

FIGURE 9. The D *vs.* F curves for several values of$A$ and C. Each particle is elastic, having a Poisson's ratio $\sigma = 0$.

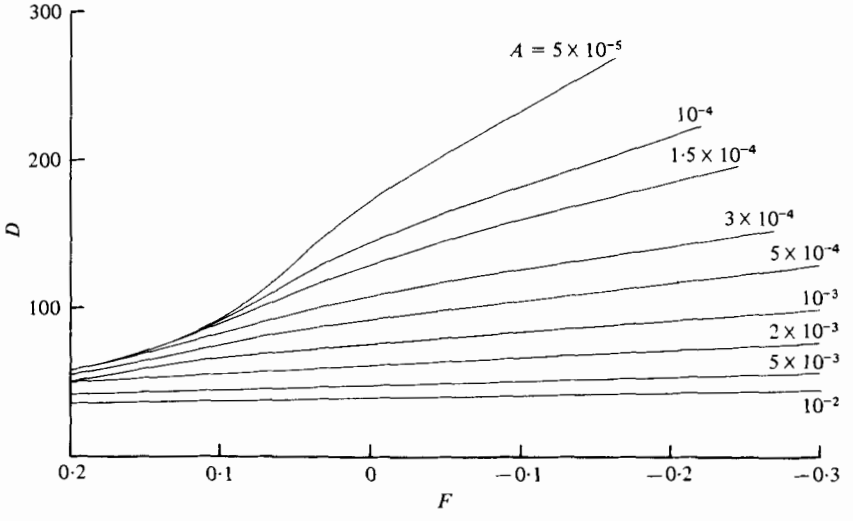

FIGURE 10. The D *vs.* F curves for several constant values of A and C. Each particle is elastic, having a Poisson's ratio $\sigma = \frac{1}{4}$.

to a given elastic sphere is not unique. It is clear that the behaviour of an elastic sphere cannot be precisely represented by the Lighthill–Fitz-Gerald model. Of course, this does not rule out the possibility that their model may represent other particles or flow geometry more accurately.

This research was supported by the U.S. National Institutes of Health through Grant HL-16851.

REFERENCES

CAMERON, A. 1966 *Principles of Lubrication*. Wiley.

FITZ-GERALD, J. M. 1969 Mechanics of red-cell motion through very narrow capillaries. *Proc. Roy. Soc.* B **174**, 193–227.

GOLDSMITH, H. L. & SKALAK, R. 1975 Hemodynamics. *Ann. Rev. Fluid Mech.* **7**, 213–297.

LIGHTHILL, M. J. 1968 Pressure forcing of tightly-fitting pellets along fluid-filled elastic tubes. *J. Fluid Mech.* **34**, 113–143.

LOVE, A. E. H. 1944 *A Treatise of the Mathematical Theory of Elasticity*, 4th edition. Dover.

SKALAK, R., CHEN, P. H. & CHIEN, S. 1972 Effect of hematocrit and rouleaux on apparent viscosity in capillaries. *Biorheol.* **9**, 67–82.

TÖZEREN, H. & SKALAK, R. 1978 The steady flow of closely fitting incompressible elastic spheres in a tube. *J. Fluid Mech.* **87**, 1–16.